Formation of Earth-sized planets within the Kepler-1647 system habitable zone

G. O. Barbosa [1,2]★ O. C. Winter [2] A. Amarante [2,3,4] and E. E. N. Macau [1,5]

[1] *Laboratório de Computação Aplicada, National Institute for Space Research (INPE), São José dos Campos, SP 12227-010, Brazil*
[2] *Grupo de Dinâmica Orbital e Planetologia, São Paulo State University (UNESP), Guaratinguetá, SP 12516-410, Brazil*
[3] *State University of Mato Grosso do Sul (UEMS), Cassilândia, MS 79540-000, Brazil*
[4] *Federal Institute of Education, Science and Technology of São Paulo (IFSP), Cubatão, SP 11533-160, Brazil*
[5] *Federal University of São Paulo (UNIFESP), Institute for Science and Technology, São José dos Campos, SP 12247-014, Brazil*

ABSTRACT

The *Kepler-1647* is a binary system with two Sun-type stars ($\approx$1.22 and $\approx$0.97 M$_\odot$). It has the most massive circumbinary planet ($\approx$1.52 M_{Jup}) with the longest orbital period ($\approx$1107.6 d) detected by the *Kepler* probe and is located within the habitable zone (HZ) of the system. In this work, we investigated the ability to form and house an Earth-sized planet within its HZ. First, we computed the limits of its HZ and performed numerical stability tests within that region. We found that HZ has three subregions that show stability, one internal, one co-orbital, and external to the host planet *Kepler-1647b*. Within the limits of these three regions, we performed numerical simulations of planetary formation. In the regions inner and outer to the planet, we used two different density profiles to explore different conditions of formation. In the co-orbital region, we used eight different values of total disc mass. We showed that many resonances are located within regions causing much of the disc material to be ejected before a planet is formed. Thus, the system might have two asteroid belts with *Kirkwood gaps*, similar to the Solar system's main belt of asteroids. The co-orbital region proved to be extremely sensitive, not allowing the planet formation, but showing that this binary system has the capacity to have Trojan bodies. Finally, we looked for regions of stability for an Earth-sized moon. We found that there is stability for a moon with this mass up to 0.4 Hill's radius from the host planet.

Key words: planets and satellites: formation – binaries: close.

1 INTRODUCTION

Often several exoplanets are discovered and confirmed in the most diverse dynamic conditions. Planets in binary systems are one of those exotic cases. Today they count 150 exoplanets in 102 systems (current data from the catalogue presented in Schwarz et al. 2016). These exoplanets are distributed in two types of orbits: (1) *P-type*: systems where the planet is orbiting the binary pair. It receives this name because it has a planet-like orbit, that is, it orbits the centre of mass of the system and (2) *S-type*: systems where the planet orbits only one of the binary components. This type of orbit gets its name because it does not orbit the centre of mass, but one of the bodies of the system as a satellite (Dvorak 1982).

Even with this expressive number of exoplanets confirmed in binary systems, none of them are terrestrial. In the other hand, in the case of short-period binary systems, or close binaries as they are also known, some works have already shown numerically that terrestrial planets can be formed (Lissauer et al. 2004; Quintana & Lissauer 2006). In Barbosa et al. (2020), the possibility of Earth-sized planets being formed within their habitable zones (HZ) has been investigated. Among all systems studied in this work, it is shown that *Kepler-35* (Welsh et al. 2012) and *Kepler-38* (Orosz et al. 2012b) systems are

the ones with the greatest capacity for this to occur. These results show that the non-existence of a terrestrial planet in binary systems is more associated with the difficulty of discovering these planets in comparison to the gas giants.

The HZ of a system is the region around a star where a terrestrial mass planet with a CO_2–H_2O–$0N_2$ atmosphere can sustain water in its liquid form on its surface (Huang 1959; Hart 1978; Kasting, Whitmire & Reynolds 1993; Underwood, Jones & Sleep 2003; Kaltenegger & Sasselov 2011). This broad definition can be extended both to systems with only one star and to multiple-star systems. In Haghighipour & Kaltenegger (2013), a methodology was developed to calculate the limits of this region in binary systems with planets in *P-type* orbits following the model proposed in Kopparapu et al. (2013a, b). This method finds the limits of HZ for an Earth-type planet, that is, a gas giant in the same region cannot be considered habitable. This occurs with some planets, such as *Kepler-16b* (Doyle et al. 2011), *Kepler-47c,d* (Orosz et al. 2012a, 2019), and *Kepler-1647b* (Kostov et al. 2016), gas giants within the HZ of their systems.

In Barbosa et al. (2020), it was investigated for a set of circumbinary systems (CB) with planets already detected, whether they could form an Earth-type planet within their HZs. However, the *Kepler-1647* system, given its complexity of regions to be studied, has not been investigated. The planet of the system, *Kepler-1647b* as is it known, is the most massive CB planet ever discovered by the *Kepler* probe, with $\approx$1.5 mass of Jupiter. In addition, it has a very long

orbital period ($\approx$1100 d), which is also the longest. The planet is around a binary pair consisting of two solar mass stars that have an orbital period of approximately 11 d (Kostov et al. 2016). It has a large semimajor axis of about 2.7 au, which places it within the conservative HZ of the system (Barbosa et al. 2020), being the widest HZ among all CB planetary systems discovered by the *Kepler* probe.

As the system has the *Kepler-1647b* planet formed, we will consider that the gas disc has already been dissipated in the process of forming this gaseous giant, following the conventional model that terrestrial planets are formed after this phase by accretion of the remaining material of this period (Safronov 1972; Lissauer 1993). Thus, the main objective of this work is to study through numerical simulations the possibility of an Earth-sized planet be formed inside its HZ. This work was planned in order to make the most complete exploration in terms of initial conditions. As the planet *Kepler-1647b* is close to the centre of the HZ, we divided the space of initial conditions into four parts: the regions interior and exterior to the orbit of the planet, the region co-orbital to the planet, and also the satellite region, orbiting around the planet. And in all cases were performed representative sets of simulations that lead to reliable conclusions. The structure of the manuscript is: in Section 2, the HZ of the *Kepler-1647* system was calculated. In Section 3, we carry out a stability test within the HZ of this system by means of numerical simulations using test particles. In Section 4, we study the last stage of planetary formation within the stable regions found in Section 3. In Section 5, again through computer simulations, we looked for the stability limits of a moon with a mass equal to that of the Earth around the planet *Kepler-1647b*. Finally, we conclude our work in Section 6 emphasizing the main results.

2 KEPLER-1647 HABITABLE ZONE

The planet *Kepler-1647b* has many details that make it stand out in comparison to the other circumbinary planets (CBP) already confirmed, at least so far. One of them is its mass of $\approx$1.5 M_{jup}, which puts it as the most massive. Another odd detail is its longest orbital period of all, with a semimajor axis of $\approx$2.72 au its orbital period is 1107.59 d (Kostov et al. 2016). The system's stars are also the most massive among CB systems with planets detected by the *Kepler* probe (Borucki et al. 2010) and its *K2* upgrade (Howell et al. 2014). Both have around a solar mass and complete a period in 11 d with a moderate eccentricity ($e_{bin} = 0.16$). For more details of the system, check Table 1. The luminosity of the stars shown in this table was calculated using

$$\frac{L}{L_\odot} = \left(\frac{R}{R_\odot}\right)^2 \left(\frac{T}{T_\odot}\right)^4, \tag{1}$$

where L, T, and R represent the luminosity, effective temperature, and radius of the star to be calculated, respectively, and $L_\odot$, $R_\odot$, and $T_\odot$ are the luminosity, radius, and effective temperature of the Sun (Duric 2004).

In the last decade, together with the confirmation of planets in binary systems, many works have endeavoured to know the conditions and limits of the HZ of these systems (Eggl et al. 2012, 2013; Kane & Hinkel 2012; Quarles, Musielak & Cuntz 2012; Haghighipour & Kaltenegger 2013; Kaltenegger & Haghighipour 2013; Liu, Zhang & Zhou 2013; Mason et al. 2013, 2015; Müller & Haghighipour 2014; Zuluaga, Mason & Cuartas-Restrepo 2016).

In this work, to calculate the HZ limits of the *Kepler-1647* system, we used a model proposed by Haghighipour & Kaltenegger (2013). Its work generalizes the calculation of the HZ limits to an Earth-type planet defined in Kopparapu et al. (2013a, b) for binary systems with

Table 1. Mutual inclination refers to the inclination between the planet and the binary stars.

Binary star data		
Primary mass, M_A	1.221	$M_\odot$
Secondary mass, M_B	0.968	$M_\odot$
Primary radius, R_A	1.790	$R_\odot$
Secondary radius, R_B	0.966	$R_\odot$
Primary temperature, T_A	6210	K
Secondary temperature, T_B	5770	K
Primary luminosity,[a] L_A	4.269	$L_\odot$
Secondary luminosity,[a] L_B	0.927	$L_\odot$
Orbital period	11.259	d
Semimajor axis, a_{bin}	0.128	au
Eccentricity, e_{bin}	0.160	
Planet data		
Orbital period	1,107.592	d
Semimajor axis, a_p	2.721	au
Eccentricity, e_p	0.058	
Mutual inclination	2.985	°
Mass	1.520	M_{jup}
Reference	Kostov et al. (2016)	

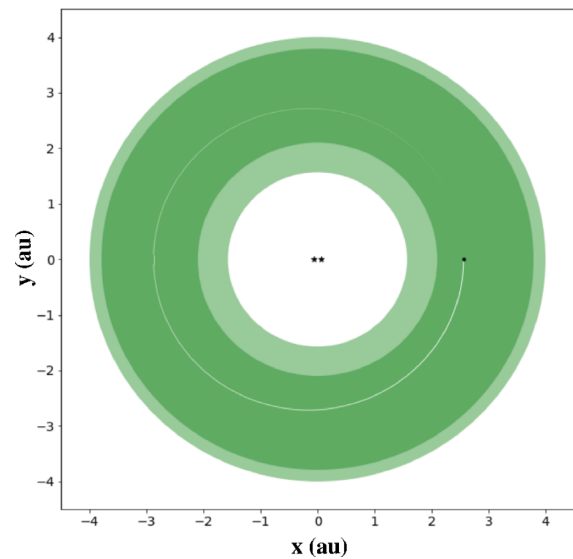*Note.* [a]The star's luminosity was calculed using equation (1).

Figure 1. Orbital plane of the binary pair of the *Kepler-1647* system showing its HZ limits. The extended and conservative HZ (Kopparapu et al. 2013a, b) are represented in light and dark green. The figure is centred on the centre of mass of bodies (stars and planet). The black stars in the centre represent the stars of the system and the point with the white trail the planet *Kepler-1647b*.

Table 2. *Kepler-1647* HZ boundaries.

	Conservative HZ		Extended HZ	
	Inner (au)	Outer (au)	Inner (au)	Outer (au)
Kepler-1647	2.10	3.79	1.57	4.00

planets in *P*-type orbits. Fig. 1 shows the HZ of the system and its limits can be seen more precisely in Table 2. In this Figure, the stars are in the centre and the planet is orbiting within the HZ with the trace of its orbit in white. It is important to remember that even though it

Table 3. Initial conditions of the massless particles for stability test.

Number of particles	10 000	
Inner limit (with −20 per cent)	1.081	au
Outer limit (with +20 per cent)	4.486	au
Inclination	10^{-5} to 10^{-4}	deg
Eccentricity	0.0–0.01	

is within the HZ, the planet cannot be considered habitable due to the fact that these limits are calculated for an Earth-type planet.

3 HZ STABILITY TEST

Before performing any numerical simulation of planetary formation, we need to investigate the stability of the system. The stability we are referring to is the location where particles survive within the HZ for more than 1 Myr, that is, they are not ejected out of that region neither collide with the stars nor the planet. In the work of Quarles et al. (2018), the authors studied the limits of stability of the CB planets confirmed by the *Kepler* mission. They showed that the greater the eccentricity of the binary pair, the farther from the stars is the inner stability limit. In the case of the *Kepler-1647* system, they have shown that the a_c limit is 0.3497 au. The same is shown in Pichardo, Sparke & Aguilar (2005, 2008), looking for '*invariant loops*' using test particles, it is shown that the size of the stable disc around the stars decreases according to the increase of the eccentricity of the binary stars.

Bearing in mind that the planet *Kepler-1647b* has a semimajor axis equal to 2.721 au, there is a large region between this limit of internal stability up to the planet. For this reason, Kostov et al. (2016) also checked the conditions for a hypothetical planet (with the same mass of the *Kepler-1647b*) to be stable in that region using Mean Exponential Growth factor of Nearby Orbits (MEGNO) formalism (Goździewski et al. 2001; Cincotta, Giordano & Simó 2003; Hinse et al. 2015). The authors have found that there is a stable region from ≈0.5 to ≈2.0 au.

In our work, as we are interested in exploring the formation of an Earth-sized planet within the HZ, we need to investigate stability throughout this region. Our goal here is to find the limits of stability so that later we can carry out the simulations of planetary formation. For this, we performed numerical simulations using MINOR-MERCURY package, an adaptation of the MERCURY package (Chambers 1999), with option for close binaries made by us following Chambers et al. (2002), which was extensively tested in Barbosa et al. (2020).

3.1 Initial conditions

As we are interested in exploring the formation of an Earth-sized planet within the HZ, we will investigate the stability of the system within this region +20 per cent (Table 3). For this, we used massless particles that interact gravitationally only with the host planet and the stars of the system, that is, without mutual interaction between them. Particles were randomly distributed between the internal and external limits with an extra margin of 20 per cent of the entire width of the extended HZ. For more details, see Table 3.

The initial eccentricity of each particle varied between 0.0 and 0.01 and the initial inclination between 10^{-5} and 10^{-4} deg. We despise the fact that the planet is within HZ to study the stability limit around it and also to investigate possible stability in its co-orbital region.

Thus, in our simulations are present the stars, the host planet of the Kepler-1647 system with all its real data that can be checked in Table 1, and the test particles. Ejection is considered to be particles exceeding 10 au from the centre of mass of the system or exceeding the interior stability limit ($a_c = 0.3497$ au) shown in Quarles et al. (2018). The length of simulation time is 1 Myr.

3.2 Results

Fig. 2 shows the dynamic evolution of particles over time. As expected, we can note that the host planet, with more than 1.5 M_{jup}, produces a lot of disturbance in the disc. Its presence makes particles close to it to have a considerable increase in eccentricity in the first thousands of years of simulation. This increase causes the particles to cross the planet's orbit, colliding with it or being ejected from the system. From the initial 10 000 particles, 55 per cent are ejected and 0.5 per cent collide with the planet. The outermost regions of the disc have the particles with the largest eccentricity.

At the end of the simulation (Figs 2 and 3), we have that it can be divided into three stable subregions (at least), one internal to the planet, one coorbital, and one external to it. In this way, there are three regions where we can explore the planetary formation. The stability limits of the co-orbital region needed to be studied in more detail, and this will be discussed in the next subsection. However, the limits of the internal and external regions of the planet can be seen in Fig. 3. The dashed magenta lines show the limits where they are and will be used to distribute the disc of matter for the study of planetary formation.

3.3 Co-orbital stability

Particles in the co-orbital region share the same orbit with the CB planet, close to the stable Lagrangian equilibrium points L_4 and L_5. We note in Fig. 3 a considerable volume of remaining particles in this region. Since these orbits are extremely sensitive and unknown in binary systems, we are going to show here the study of this particular region in more detail.

As these regions close to the equilibrium points are symmetrical, we perform this test only around the point L_4 and the results found for it will be similar for L_5. 5000 particles were distributed between 2.22 and 3.22 au, corresponding to twice the largest width of the horseshoe orbit given by

$$\Delta_{\text{horse}} = \mu^{\frac{1}{3}} a_p, \tag{2}$$

(Dermott & Murray 1981) where μ is the relative mass and a_p the semimajor axis of the *Kepler-1647b*. The eccentricity and inclination used was the same of the planet co-orbital to them. We use these values because the secular perturbations caused by the planet in the particles force them to have the same eccentricity and inclination as itself (Murray & Dermott 1999). Check Table 4 for more details on initial conditions of the simulation. The particles only interact gravitationally with the stars and the planet; there is no mutual interaction among them. The length of integration time is also 1 Myr.

Fig. 4 shows the result of the simulation. From the initial 5000 particles, 472 survived. In Fig. 4(a) the initial position of the particles in Cartesian *x* and *y* coordinates is shown, and in Fig. 4(b), the initial condition of the surviving particles at the end of the integration is shwon. This result shows that even though the system is binary, there is a considerable stable region. We will use the orbital elements of the surviving particles to test the planetary formation in this region.
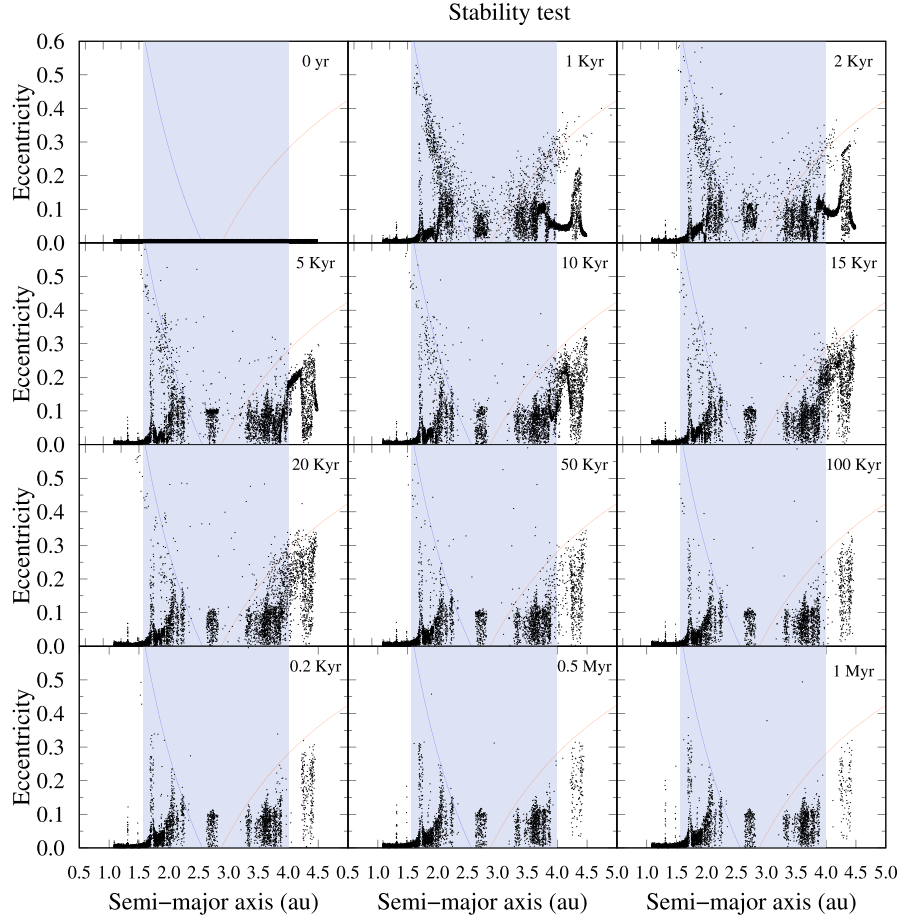
Stability test

Figure 2. Snapshots in time of the dynamic evolution of test particles in the HZ. The horizontal and vertical axes are the semimajor axis and the eccentricity, respectively. The black dots are the particles and red lines represent the apocentre of the host planets of the system in function of the pericentre of the particle, given by $a = [a_p(1 + e_p)]/(1 - e)$, and the blue lines represent the pericentre of the planet as a function of the apocentre of the particles, given by $a = [a_p(1 - e_p)]/(1 + e)$. Where a_p and e_p are the semimajor axis and eccentricity of the planet, respectively. The shaded region in blue represents HZ of the system.
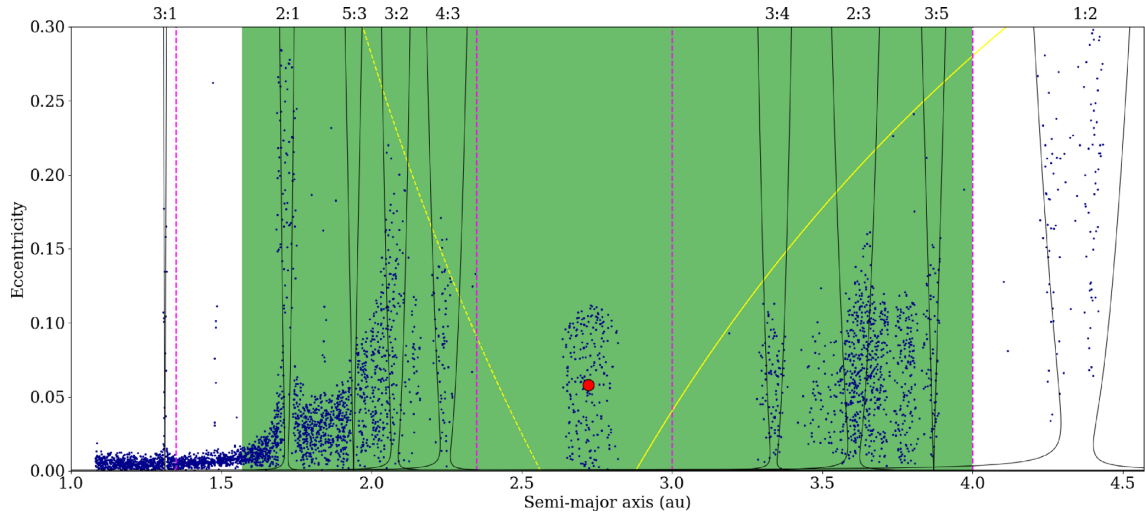

Figure 3. The final state of the test particles and the planet in 1 Myr showing the eccentricity versus the semimajor axis. The blue dots represent the particles and the red dot the planet. Yellow solid line represents the apocentre of the host planet of the system in function of the pericentre of the particles, given by $a = [a_p(1 + e_p)]/(1 - e)$, and the yellow dashed line represents the pericentre of the planet as a function of the apocentre of the particles, given by $a = [a_p(1 - e_p)]/(1 + e)$, where a_p and e_p are the semimajor axis and eccentricity of the planet, respectively. The shaded region in green denotes the HZ. The dashed magenta lines indicate the initial position limits of particles for the planetary formation simulations. The black lines denote the maximum libration zones as a function of semimajor axis and eccentricity for a selection of resonances. The nominal resonance locations are indicated on the top of the plot.

Table 4. Parameters of the stability test in the co-orbital region.

	Values	Unit
Number of particles	5000	un
Semimajor axis (min)	2.220	au
Semimajor axis (max)	3.220	au
Eccentricity	0.058	
Inclination	2.986	deg
Mean anomaly (min)	0	deg
Mean anomaly (max)	180	deg

4 PLANETARY FORMATION

The stability test provided us with three different scenarios to explore the planetary formation in this system. Being an internal region, a coorbital, and one external to the host planet. Therefore, we set-up a set of simulations for these three cases.

4.1 Co-orbital region

Studies of the formation of terrestrial planets in co-orbital regions have already been explored in one-star systems. In Beaugé et al. (2007), the authors numerically investigated different scenarios for the formation of terrestrial planets using a hypothetical system with a planet similar to Jupiter orbiting a Sun-like star. In their simulations, an *N*-body integrator, the authors showed that it is not possible to form a Trojan planet with a mass larger than 0.6 $M_{\oplus}$. With a different context, Izidoro, Winter & Tsuchida (2010) also numerically explored the formation of smaller bodies in the co-orbital region of a satellite orbiting a planet. The work of Liberato & Winter (2020) studied the structure of co-orbital stable regions for a wide range of mass ratio systems and provide empirical equations to describe them.

We began our study by assuming that particles with mass are trapped around what would be the L_4 point of Lagrangian equilibrium in a Solar type system. As we can see in the stability test shown in the previous section, there is a stable portion sharing the orbit with the host planet, like the Trojans in the case of the Solar system. Thus, taking into account the stability found, we studied the possibility of a larger body being formed in this region. As it is a very sensitive region from a dynamic point of view, we explore different mass values around this region.

4.1.1 Initial conditions

In order to explore this region to the full, we used eight different total mass values, being 0.4, 0.6, 0.8, 1.0, 1.2, 1.4, 1.6, and 1.8 $M_{\oplus}$.
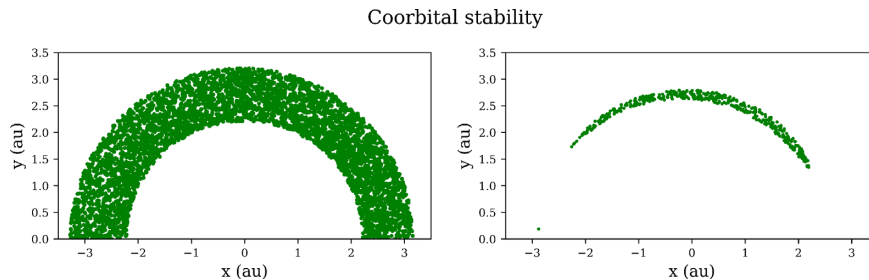
Mass distribution in coorbital region
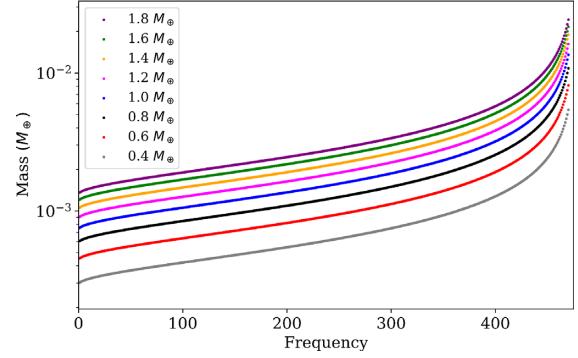
Figure 5. Mass distribution of particles for different values of total mass.

In all of these cases, we used the initial positions of the surviving particles from the stability test in the co-orbital region (see Fig. 4). The eccentricities and inclinations of the particles were also kept the same used in the stability test of the co-orbital region, which are, the same as the host planet. However, as we are now interested in bodies that increase mass and can become planets, all bodies interact gravitationally with each other. In the simulations, we have the two stars, the host planet, and the particles.

For each of these total mass values, we performed 10 different simulations, resulting in 80 simulations, where we randomly vary their masses. With the eight different values of total mass, we distributed the particle's masses following a power law. In all distributions, there is a large amount of less massive particles than particles with a higher mass (see Fig. 5).

The power law used was

$$m_p(\delta_i) = MT_j(\alpha + \beta \sqrt{\delta_i})^{\gamma}, \tag{3}$$

where m_p, MT_j ($j = 1, 2, ..., 8$), and δ_i ($i = 1, 2, ..., 471$) represent the individual mass of each particle, the total mass, and the frequency of distribution, respectively. The values of α, β, and γ are constant coefficients equal to 0.60318E+14, −0.27616E+13, and −0.59436 found numerically. The simulations were carried out by 200 Myr.

4.1.2 Results

As mentioned in previous sections, we performed numerical simulations using as initial conditions the initial positions of the surviving particles in the co-orbital region stability test. 10 simulations were performed for each total mass value, totaling 80 simulations. Next, we will show the results of each of these simulations.

As an analysis of the results, we defined an Earth type planet being a body with a mass close to that of Earth and within HZ. A

Coorbital stability

Figure 4. The two subfigures show the positions of the particles in Cartesian *x* and *y* coordinates. In (a) all 5000 particles are present in their initial positions and in (b) the initial positions of the surviving particles.

Table 5. The columns show from left to right the identification number of the simulation, the number of surviving bodies, the surviving particle with the greatest mass and the semimajor axis, the eccentricity and inclination of this particle, and its mass.

						Results of simulations of planetary formation in the co-orbital region						
Sim	SP	Particle	a_f (au)	e	i (deg)	Mass ($M_\odot$)	Sim	SP	Particle	a_f (au)	e	i (deg)	Mass ($M_\odot$)
0.4–1	2	part4876	2.7843	0.0693	2.7694	7.6841e-4	1.2–1	2	part1973	2.7158	0.0897	2.6444	7.0423e-3
0.4–2	5	part4541	2.6778	0.1353	2.8524	1.7559e-3	1.2–2	2	part901	2.7263	0.1269	4.4843	2.0590e-3
0.4–3	2	part1109	2.7547	0.0688	3.5176	1.2799e-2	1.2–3	2	part4876	2.6747	0.1215	3.9838	6.6946e-3
0.4–4	3	part452	2.6908	0.0794	2.8596	8.2690e-3	1.2–4	3	part2747	2.6887	0.0946	2.5085	4.0041e-2
0.4–5	2	part1734	2.7150	0.0643	2.9806	1.0349e-2	1.2–5	2	part3443	2.6745	0.0633	3.1422	2.6919e-2
0.4–6	2	part3570	2.7107	0.0136	1.8376	7.4712e-3	1.2–6	3	part4876	2.7554	0.0499	4.0617	1.9971e-2
0.4–7	3	part3073	2.7660	0.0895	3.1394	8.3442e-3	1.2–7	3	part2847	2.7431	0.0583	4.1182	2.7428e-3
0.4–8	2	part2434	2.7509	0.0516	1.8793	4.5088e-3	1.2–8	3	part890	2.6683	0.0770	4.1952	1.2612e-2
0.4–9	2	part3124	2.7524	0.0334	3.4045	8.0364e-3	1.2–9	2	part1942	2.6940	0.0241	3.4894	1.2600e-2
0.4–10	2	part3224	2.7696	0.0352	2.8087	2.0903e-2	1.2–10	2	part2128	2.7333	0.0501	3.3821	1.2477e-2
0.6–1	2	part2922	2.7097	0.0958	2.2859	6.2828e-3	1.4–1	3	pt2192	2.7348	0.0707	6.8415	2.1837e-2
0.6–2	5	part805	2.6854	0.0666	3.4304	1.5242e-3	1.4–2	3	part1180	2.6942	0.1053	3.7177	1.7488e-2
0.6–3	3	part2921	2.7064	0.1253	3.3277	4.5469e-3	1.4–3	3	part1761	2.7285	0.0476	3.8518	1.3281e-2
0.6–4	2	part4372	2.7455	0.0599	3.5614	1.6173e-2	1.4–4	2	part720	2.7154	0.0408	1.9427	2.6899e-2
0.6–5	2	part2704	2.6696	0.0695	2.7640	2.3414e-2	1.4–5	3	part1251	2.7901	0.05868	2.6928	2.8419e-2
0.6–6	3	part3222	2.7483	0.0445	2.118	8.9929e-3	1.4–6	3	part3813	2.6856	0.04263	2.4857	2.6621e-3
0.6–7	3	part2929	2.7227	0.0509	2.5468	8.6247e-3	1.4–7	3	part3321	2.7266	0.0544	3.9329	4.2609e-2
0.6–8	2	part3542	2.6896	0.1053	3.4187	5.6994e-3	1.4–8	1	part2718	2.7370	0.0667	2.9659	3.0811e-2
0.6–9	2	part1009	2.6966	0.0934	3.3951	9.5336e-3	1.4–9	2	part1238	2.7256	0.0608	4.0384	1.2338e-2
0.6–10	3	part261	2.7113	0.1026	2.9009	4.4257e-3	1.4–10	2	part1694	2.6729	0.0468	2.6681	6.0304e-3
0.8–1	2	part3035	2.7007	0.0772	3.0358	1.4528e-2	1.6–1	2	part1399	2.7238	0.0524	2.0200	3.3219e-2
0.8–2	3	part4173	2.7853	0.0878	3.5697	1.2905e-2	1.6–2	2	part2070	2.7340	0.0433	3.9092	8.6235e-3
0.8–3	2	part3375	2.6840	0.0064	2.8048	1.0228e-2	1.6–3	4	part2805	2.6834	0.0835	0.7809	3.8656e-3
0.8–4	5	part1055	2.6944	0.1293	3.5695	2.4642e-3	1.6–4	3	part560	2.8057	0.0660	4.0955	7.6440e-3
0.8–5	5	part1734	2.7432	0.0183	3.1201	1.2049e-2	1.6–5	2	part3756	2.7329	0.0564	2.9696	2.6583e-2
0.8–6	2	part1966	2.7460	0.0452	3.7021	1.0597e-2	1.6–6	3	part2320	2.7278	0.0725	2.8423	1.3899e-2
0.8–7	3	part1655	2.6967	0.0514	3.8889	3.6993e-3	1.6–7	1	part3280	2.6796	0.0324	3.0362	1.3260e-2
0.8–8	2	part3331	2.7358	0.0384	2.5727	5.1276e-3	1.6–8	2	part158	2.7225	0.1061	1.5238	1.9593e-2
0.8–9	2	part2896	2.6666	0.0447	3.6505	4.6755e-3	1.6–9	2	part2558	2.7816	0.0576	2.1428	2.0084e-2
0.8–10	3	part1753	2.7214	0.0684	2.6985	1.1620e-2	1.6–10	3	part471	2.7412	0.0687	2.3680	2.5096e-2
1.0–1	3	part4815	2.7005	0.0646	3.2192	4.9347e-3	1.8–1	3	part2998	2.7643	0.0804	2.1566	2.4359e-3
1.0–2	2	part4557	2.7178	0.0815	1.8794	1.3740e-2	1.8–2	2	part733	2.7455	0.0743	3.6756	4.2858e-3
1.0–3	3	part1109	2.7128	0.0165	2.1330	5.9580e-3	1.8–3	3	part541	2.7006	0.0626	2.5949	3.4212e-2
1.0–4	3	part2095	2.6467	0.0518	2.5262	3.1756e-3	1.8–4	2	part3443	2.6908	0.1019	1.0418	3.0506e-3
1.0–5	2	part2704	2.7453	0.0348	3.2974	1.6286e-2	1.8–5	2	part1646	2.7357	0.1122	2.5803	6.0330e-2
1.0–6	2	part3222	2.6792	0.0590	2.9855	8.9929e-3	1.8–6	2	part4042	2.7477	0.1008	3.3634	2.1837e-2
1.0–7	2	part2921	2.7388	0.0986	2.8586	5.8992e-3	1.8–7	3	part4550	2.7310	0.0095	3.1216	3.6401e-2
1.0–8	3	part4500	2.6878	0.1181	4.3627	1.3708e-3	1.8–8	3	part4098	2.7412	0.0544	3.1086	7.5901e-2
1.0–9	3	part582	2.7952	0.0588	2.9855	8.9929e-3	1.8–9	2	part1399	2.7198	0.0515	1.1901	1.7153e-2
1.0–10	2	part2138	2.6847	0.0585	3.2003	9.6590e-3	1.8–10	1	part4525	2.7431	0.0916	3.5973	8.4359e-3

first analysis of our results show that in none of the simulations an Earth-type was formed. Table 5 shows the results found over 200 Myr of the simulations with total masses from 0.4 to 1.8 Earth masses. The first column indicates the simulation id, composed of *XX-Y*, *XX* being the total mass and *Y* the number of the simulation, which varies from 1 to 10.

The region co-orbital to a planet is recognized as a sensitive region from stability in Solar type systems. In the case of binary systems, this region is even more sensitive as we can see from Table 5, where few bodies survive the simulation and there is practically no mass addition. On the other hand, we can note that in all cases with different values of the total mass, bodies survived. This shows us that CB systems can have Trojan asteroids as in the case of the Solar system.

4.2 Inner and outer regions of the planet

As shown in Fig. 3, in addition to the co-orbital region, two others have some stability, an internal and an external region. In order to explore the terrestrial planetary formation in these regions, we performed 40 simulations with different initial conditions. In all of them, we again use our numerical package adapted with the option for close-binary systems. The largest and which has the largest number of particles that survive the stability test is the internal one. Besides, the beginning of the internal part demonstrates that the HZ surviving particles have less eccentricity than the outer region. In all simulations, the binary pair and the giant planet of the system will be present in addition to the circumbinary disc of matter. The data of the host bodies of the system are the real ones found in the literature and can be checked in Table 1.
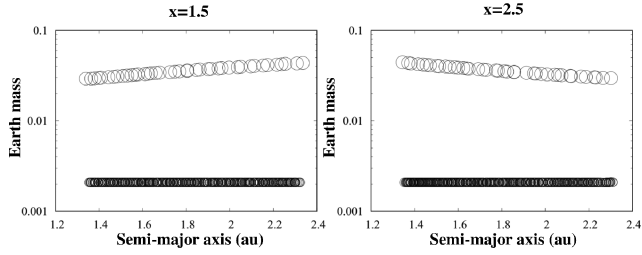
Figure 6. Initial distribution of embryos and planetesimals in the internal stable region. On the left, the mass distribution is shown using the coefficient $x = 1.5$, while on the right $x = 2.5$.
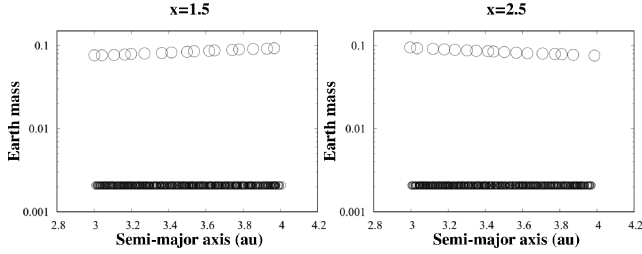

Figure 7. Initial distribution of embryos and planetesimals in the external stable region. On the left, the mass distribution is shown using the coefficient $x = 1.5$, while on the right $x = 2.5$.

4.2.1 Initial conditions

To explore the planetary formation in these two regions, we used a protoplanetary discs with bimodal mass distribution composed of planetesimals and planetary embryos, resulting from the runaway and oligarchic growths, as shown by Kokubo & Ida (1998, 2000). Following this context, the mass of the total planetesimals represents 40 per cent of the total mass of the disc while the sum of the masses of the embryos the other 60 per cent. The major role of planetesimals is to provide dynamic friction to dump the variation of eccentricities and inclinations of planetary embryos (O'Brien, Morbidelli & Levison 2006; Morishima et al. 2008). The internal disc has a width of 1 au and extends from 1.35 to 2.35 au and the external disc, also with 1 au wide, extends from 3 to 4 au. The individual mass of the planetesimals is ≈0.0021 $M_\oplus$ and they are distributed with a surface density profile of $\Sigma_1 r^{-x}$, where r is the radial distance and Σ_1 is a solid surface density adjusted to fill a total mass of 2.5 $M_\oplus$ within the disc. The mass of each embryo scales following:

$$M_{emb} \sim \Delta^{3/2} r^{3/2(2-x)}, \tag{4}$$

(Kokubo & Ida 2002; Raymond, Quinn & Lunine 2005), where x is a free parameter of the surface density profile and Δ the mutual separation in Hill's radius. We set Δ randomly by 5–10 Hill radii (Kokubo & Ida 2000, 2002). Given this distribution, the outer disc has more massive planetary embryos and in smaller numbers than the inner disc. We used two different values of parameter x, 1.5 and 2.5, for each disc (internal and external). In the case of $x = 1.5$, we have less massive embryos at the beginning of the disc whereas, with $x = 2.5$, it results in a more massive disc in its initial part (see Figs 6 and 7). We assume that embryos gravitationally interact with each other and with all other bodies of the system, in the case of planetesimals, they do not interact with each other but are allowed to interact with all other bodies. The eccentricity of all bodies was chosen randomly between 0 and 0.01, the orbital inclination between 10^{-4} and 10^{-3} deg, and the mean anomaly between 0 and 360 deg.

Table 6. Number of planetesimals and protoplanetary embryos distributed on the internal and external discs with the two values of the x parameter.

	Inner		Outer	
	$x = 1.5$	$x = 2.5$	$x = 1.5$	$x = 2.5$
Embryos	40	41	17	17
Planetesimals	480	480	480	480

The longitudes of the ascending nodes and the arguments of the periastron of all bodies were initialized with zero. For each of the discs, we have two distinct values of x and in each of these cases, we performed 10 simulations with slightly different initial conditions for the protoplanetary embryos and planetesimals. Thus, there is a total of 20 simulations for each disc. Table 6 shows the average number of protoplanetary embryos and planetesimals for the simulations of both discs with the two values of x. During the simulations, bodies that have a heliocentric distance of less than 0.1 au or greater than 10 au were removed from the system. All simulations were integrated by 100 Myr.

4.3 Results and discussion

Our numerical results of planetary formation are shown in Fig. 8. Two different disc mass distribution profiles were used in two regions considered stable within the HZ totalling 20 simulations, 10 with each profile in each of these regions. Thus, we will discuss the results of these simulations separately below.

4.3.1 Inner disc

As previously mentioned, 20 numerical simulations were carried out with two different mass distribution profiles within this internal region. More precisely, it extends from 1.35 to 2.35 au of the centre of mass of the system.

In this case, protoplanetary embryos are less massive than in the outer region and consequently more numerous, as can be compared in Figs 6 and 7. In the case where $x = 1.5$, the mass of the embryos is increasing along the disc, while in the case of x = 2.5, the mass is decreasing. This fact is made more important by the fact that the giant planet is present on the outer edge of the disc. Since this planet has approximately 1.5 masses of Jupiter, the disturbance caused by it on the disc is quite considerable. Fig. 8 shows that in all simulations of this region, the surviving bodies have a semimajor axis <1.7 au.

In addition to the proximity of a very massive planet, another factor that causes a lot of disruption in the disc are the internal resonances with the planet. Within this disc, four important internal resonances are located, as can be seen in Fig. 3. One being of the second-order (5:3) and other three of first-order (2:1, 3:2, and 4:3). These resonances increase the eccentricity of the bodies causing them to cross the planet's orbit. These intersections cause close encounters between the disc material and the planet, causing collisions with the planet or ejections of the bodies.

Even though the area of this disc is not large, which favours collisions taking into account the number of bodies on the disc, these resonances contribute to them being ejected before any massive body is formed. Figs 9 and 10 shows that in the first hundreds of thousands of years, the eccentricity of the bodies varies widely, going from almost circular to approximately 0.4 in 0.2 Myr. Mainly around 1.71 au, where the 2:1 internal resonance is located.
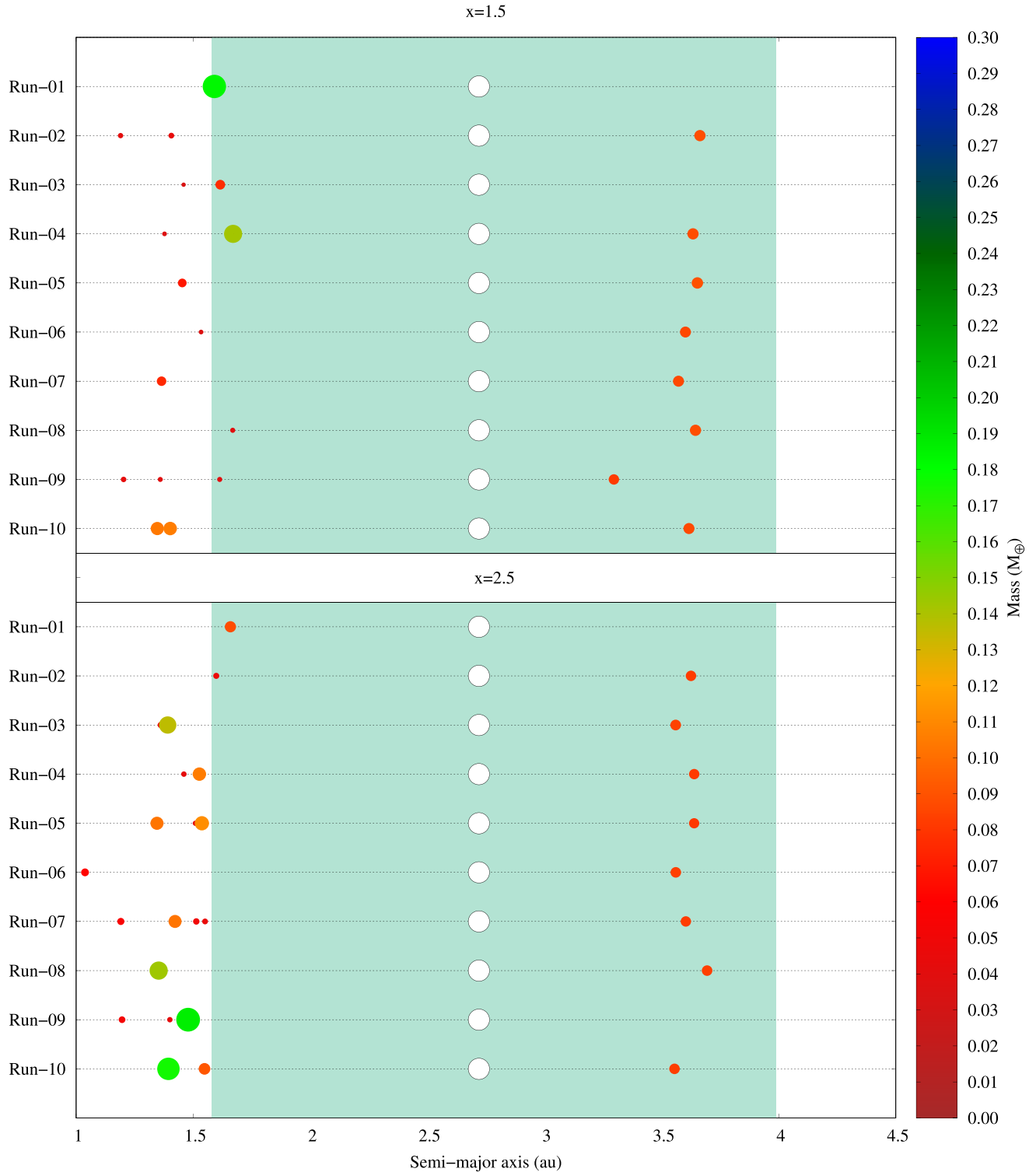
Figure 8. Final configuration of the 40 simulations performed. The figure shows the final mass of the surviving bodies in 100 Myr. In the centre in white is the host planet *Kepler-1647b* of the system in its current position. Each coloured circle represents a body and its size is relative to its mass, except for the host planet. The green shaded region represents the system's HZ.

Although the difference is small, the final mass of the disc is larger in the case where $x = 2.5$. This is due to the fact that with this profile, the most massive embryos are closer to the inner edge. In this way, they have a greater chance of surviving in the simulation. Overall, the final configurations are very similar in this region.

These results show that the effects caused by the giant *Kepler-1647b* inside the disc make it impossible for a planet with the size of the Earth to be formed inside the HZ. However, this does not prevent a planet formed in another position in the system from being placed by migratory processes within the HZ. Our stability tests and
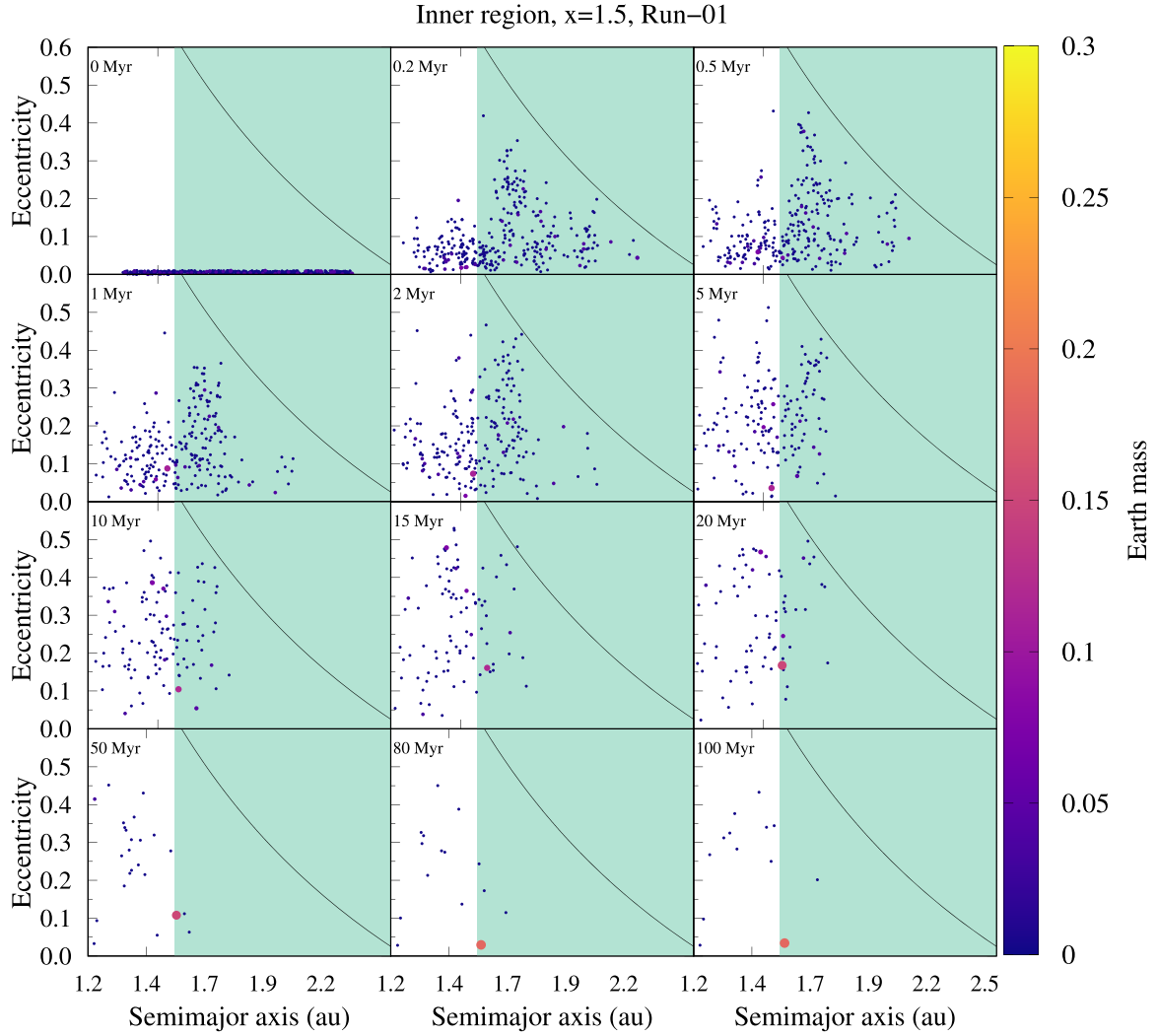
Figure 9. Snapshots in time of the dynamic evolution of protoplanetary embryos and planetesimals in the inner region with $x = 1.5$ for the case of Run-01. The horizontal and vertical axes are the semimajor axis and the eccentricity, respectively. The coloured circles represent the embryos and planetesimals and their sizes are proportional to their masses. The blue lines represent the pericentre of the planet as a function of the apocentre of the particles, given by $a = [a_p(1 - e_p)]/(1 + e)$. The shaded region in green represents HZ of the system.

planetary formation simulations show that specifically in this part of the HZ, its inner edge has stability for this to occur.

4.3.2 Outer disc

Likewise, we performed 20 simulations in the outer region, 10 of them with $x = 1.5$ and another 10 with $x = 2.5$. Despite having the same width, from 3 to 4 au, the area of this region is considerably larger, and the number of bodies within this disc is smaller.

In this case, bodies that have the smaller semimajor axis are closer to the host planet, and thus are more vulnerable to close encounters with it. The disc has three external resonances to the planet along its extension. Two of which are first-order (3:4 and 2:3) and one of second-order (3:5). These resonances contribute to the increase in the eccentricity of the disc bodies, as can be checked in Fig. 3. This increase in eccentricity causes the bodies to intersect with the apocentre of the planet, increasing the chances of close

encounters that can cause both an increase in the semimajor axis and consequently ejections as well as collisions with it.

Even though the mass is the same in the two discs, the mass distribution of the protoplanetary embryos used makes their individual mass greater and, consequently, the amount of bodies is less. This decreases the probability that collisions will occur and consequently also decrease the chances of a massive body being formed. This is because the area is considerably larger than the one previously studied, which makes the time-scale for collisions to occur to be greater. Looking in Fig. 11, we can note that most bodies are quickly ejected right at the beginning of the simulations, even before collisions occur.

Regardless of the value of parameter x, the result is quite similar, as we can check in Fig. 8. With $x = 1.5$, in two simulations (Run-01 and Run-0.3) no body survived. In all others, a protoplanetary embryo remained with its same initial mass. The same occurs with $x = 2.5$, in two simulations no body survives (Run-01 and Run-09) and in the others, only one body survived until the end of the integration.
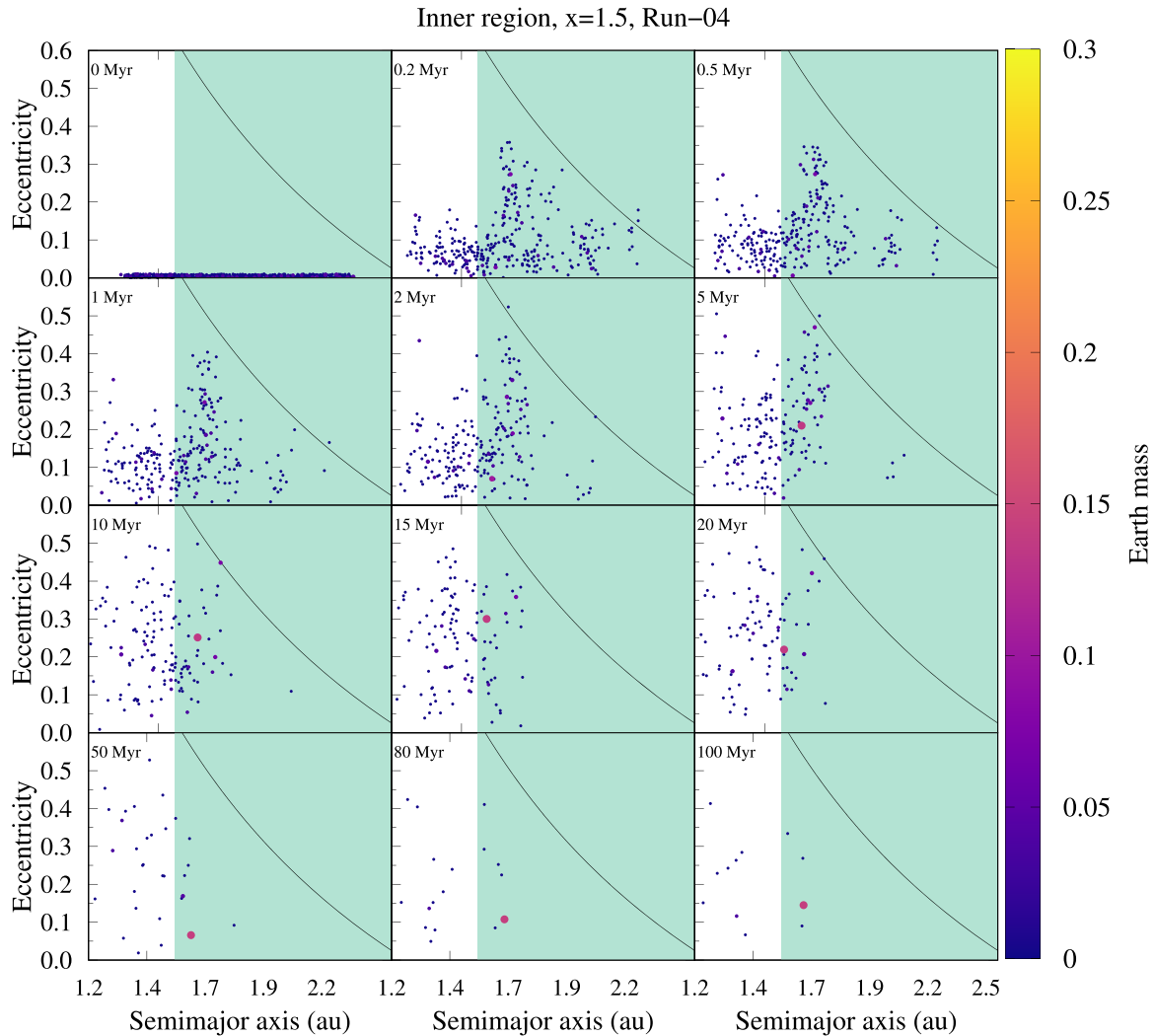
Figure 10. Snapshots in time of the dynamic evolution of protoplanetary embryos and planetesimals in the inner region with $x = 1.5$ for the case of Run-04. The horizontal and vertical axes are the semimajor axis and the eccentricity, respectively. The coloured circles represent the embryos and planetesimals and their sizes are proportional to their masses. The blue lines represent the pericentre of the planet as a function of the apocentre of the particles, given by $a = [a_p(1 - e_p)]/(1 + e)$. The shaded region in green represents HZ of the system.

Except for the simulations that no body survived and the Run-09 case with $x = 1.5$, the surviving bodies are positioned between the external resonances 2:3 and 3:5 (see Figs 3 and 8).

As in the previous disc, our results show that it is not possible to form an Earth-sized planet within this part of HZ. However, this does not prevent a planet formed in another region from being placed inside that region between the external resonances 2:3 and 3:5, in the giant's planet migratory processes.

5 STABILITY OF AN EARTH-TYPE EXOMOON

As the planet *Kepler-1647b* is within the HZ, in addition to the co-orbital bodies, its satellites or exomoons will also be. Some works have already studied the stability of an exomoon around a giant planet for long periods. In Domingos, Winter & Yokoyama (2006) through simulations of the three-body restricted elliptical problem, it is shown that a disc around a planet has an outer edge in 0.4895 Hill's radius of the host planet of the system. However, these works are for systems that have only one star.

In the work of Hamers et al. (2018), the limits of stability of a moon around CBPs discovered by the *Kepler* probe are explored. It shows that the presence of a stellar companion affects these limits and that the stability boundary is well described by the location of the 1:1 mean motion commensurability (MMC) with the stellar binary. However, it is also shown that in the case of the *Kepler-1647* system, this effect is weak because the planet's semimajor axis is large. Thus, a simplification replacing the two stars with just one with the sum of their masses, does not produce major differences in results.

Therefore, through this simplification, we performed a stability test of a planet with a mass and size equal to the Earth around the planet Kepler-1647b. For this, we use the computational package of MERCURY n-bodies (Chambers 1999) with the Bulirsch–Stoer integrator.

5.1 Numerical simulations: EXOMOON

The parameters of the stars and the host planet used in the simulations can be checked in Table 1. In each simulation, in addition to the stars and the planet, there was also a satellite (exomoon) with mass and
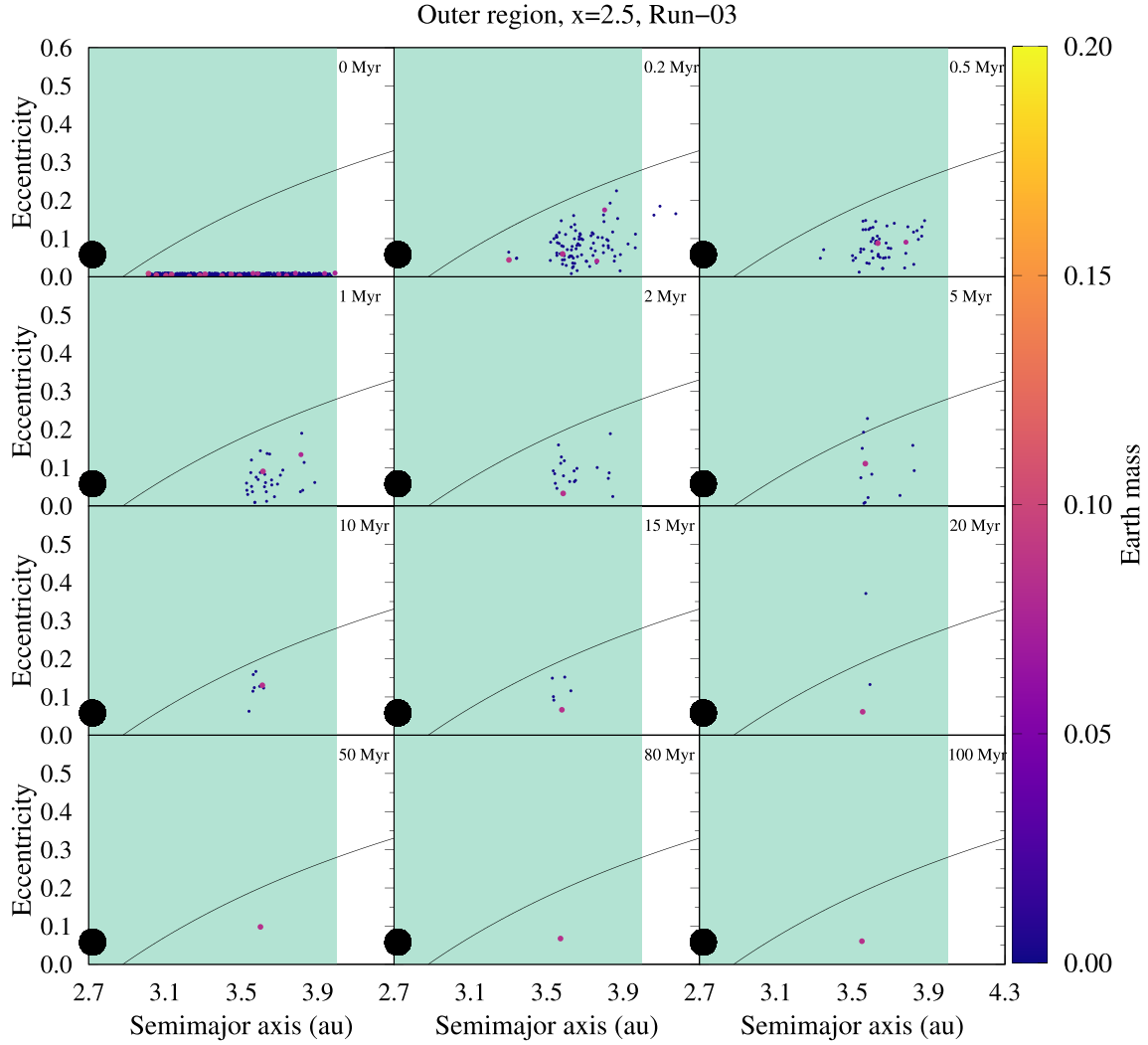
Figure 11. Snapshots in time of the dynamic evolution of protoplanetary embryos and planetesimals in the outer region with x = 2.5 for the case of Run-03. The horizontal and vertical axes are the semimajor axis and the eccentricity, respectively. The coloured circles represent the embryos and planetesimals and their sizes are proportional to their masses, except the planet that is represented in black. The black line is the apocentre of the host planet of the system in function of the pericentre of the particle, given by $a = [a_p(1 + e_p)]/(1 - e)$. The shaded region in green represents HZ of the system.

radius equal to that of Earth. We set-up a grid of eccentricity per major axis for these satellites.

The semimajor axis of the exomoons (a_{exo}) ranged from 1.5 radius of the planet (r_p) to 0.8 radius of Hill of the planet ($r_{H,p} \approx 0.165$ au) with an increment of 0.005 $r_{H,p}$. The eccentricity (e_{exo}) varied from 0.0 to 0.9 with an increase of 0.005, thus totalling 28 800 simulations. In all of them, the argument of the pericentre, ascending node, and mean anomaly elements was set equals to zero. The final simulation time was 10^4 orbital periods (≈ 650 d) of an exomoon at 1 $r_{H,p}$.

We consider as ejections in our simulations, bodies with a semimajor axis greater than 1 Hill's radius of the planet and less than 1 radius of the planet, assuming the planet as a reference centre.

5.2 Results: EXOMOON

Fig. 12 shows in black the Earth type that survived after 10^4 orbital periods. In white are the particles that have been ejected from the

system. In it, the planet *Kepler-1647b* is located at the origin. The stability limit here is approximately 0.4 Hill radii in the circular case, as can be seen in the Fig. 12. In addition, we can also perceive an island formed beyond that limit. This result, even if by approximation, shows that the planet can house a planet the same size as the Earth inside the HZ as a satellite. The origin of this planet can be due to an *in situ* formation, or even a capture.

6 FINAL REMARKS

In this work, we used numerical simulations to investigate the possibility of a planet with a mass similar to the Earth's to be formed within the HZ of the CB *Kepler-1647*. Among all the binary systems with confirmed planets, this one has the most massive with *P-type* orbit and the widest HZ. These characteristics make it one of the most complex systems of its kind and provide ample possibilities for exploring the formation of planets capable of harbouring life.
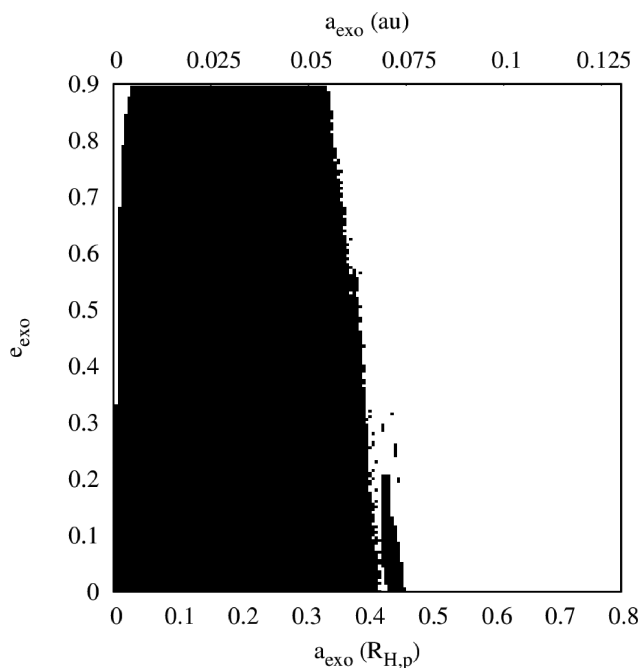
Figure 12. Simulation grid of the semimajor axis by the eccentricities of the Earth-type satellites around the planet *Kepler-1647b*. In black, they are the exomoons that survived the total integration time, while in white they are the ones that were ejected.

For this purpose, we first computed the system's HZ limits. With the limits of HZ found, the second part of our work focused on studying stability within that zone. This test showed that the system has three stable subregions within HZ. One of them internal to the planet, another co-orbital to the host planet of the system, and other external to the planet. This test shows us that there are several orbital resonances located along the particle disc. These resonances create disc gaps similar to what we see in the case of *Kirkwood gaps* (Kirkwood 1867; Dermott & Murray 1981).

As the co-orbital region has many peculiarities concerning the other two regions, we explore this subregion more fully. We used the initial conditions of the surviving particles of this specific test to perform simulations of planetary formation. Using eight values of total disc mass we ran 80 different cases, 10 for each value of total mass randomly varying the mass of the bodies by 200 Myr. The results of these simulations showed that it is impossible to form a body with a mass close to that of the Earth co-orbitally to the system planet. However, our results also show that the system has conditions to have bodies co-orbital to the planet similar to the Trojan asteroids in our Solar system.

For the other two regions, we use two distinct surface density profiles to explore planetary formation. For each distinct value of the density profile, we performed 10 simulations, totalling 40 adding the two regions. In the case that we have a disc density profile equal to 1.5, the largest planet formed was in the inner region (Run-01). This planet has approximately 0.2 masses of Earth (1.8 masses of Mars). In the event that this value is equal to 2.5, the largest planet formed is outside the HZ (0.25 Earth's mass).

As the planet is located in the centre of the HZ, a hypothetical satellite from that planet would consequently be inside the HZ. Since we have shown that a planet the size of Earth cannot form within the system's HZ, we looked for moons. Thus, we performed several computer simulations to find the possible locations where a satellite

of the Earth size can be stable. As a result, we found that the planet is capable of harbouring an Earth analogue up to approximately 0.4 Hill's radius from the centre of the planet.

Note added in proof: In the work of Georgakarakos, Eggl & Dobbs-Dixon (2021) is applied an analytical approach concerning the HZ for the *Kepler-1647* system, where they conclude that it is unlikely to host habitable worlds.

DATA AVAILABILITY

The data underlying this article will be shared on reasonable request to the corresponding author.

REFERENCES

Barbosa G., Winter O., Amarante A., Izidoro A., Domingos R., Macau E., 2020, MNRAS, 494, 1045
Beaugé C., Sándor Z., Érdi B., Süli Á., 2007, A&A, 463, 359
Borucki W. J. et al., 2010, Science, 327, 977
Chambers J. E., 1999, MNRAS, 304, 793
Chambers J. E., Quintana E. V., Duncan M. J., Lissauer J. J., 2002, AJ, 123, 2884
Cincotta P. M., Giordano C. M., Simó C., 2003, Phys. D: Nonlinear Phenom., 182, 151
Dermott S. F., Murray C. D., 1981, Icarus, 48, 1
Domingos R. C., Winter O. C., Yokoyama T., 2006, MNRAS, 373, 1227
Doyle L. R. et al., 2011, Science, 333, 1602
Duric N., 2004, Advanced Astrophysics. Cambridge Univ. Press, Cambridge
Dvorak R., 1982, Sitz.ber., Oesterr. Akad. Wiss. Math.- Nat.wiss. Kl., 191, 423
Eggl S., Pilat-Lohinger E., Georgakarakos N., Gyergyovits M., Funk B., 2012, ApJ, 752, 74
Eggl S., Pilat-Lohinger E., Funk B., Georgakarakos N., Haghighipour N., 2013, MNRAS, 428, 3104
Georgakarakos N., Eggl S., Dobbs-Dixon I., 2021, Front. Astron. Space Sci., 8, 44
Goździewski K., Bois E., Maciejewski A., Kiseleva-Eggleton L., 2001, A&A, 378, 569
Haghighipour N., Kaltenegger L., 2013, ApJ, 777, 166
Hamers A. S., Cai M. X., Roa J., Leigh N., 2018, MNRAS, 480, 3800
Hart M. H., 1978, Icarus, 33, 23
Hinse T. C., Haghighipour N., Kostov V. B., Goździewski K., 2015, ApJ, 799, 88
Howell S. B. et al., 2014, PASP, 126, 398
Huang S.-S., 1959, Am. Sci., 47, 397
Izidoro A., Winter O., Tsuchida M., 2010, MNRAS, 405, 2132
Kaltenegger L., Haghighipour N., 2013, ApJ, 777, 165
Kaltenegger L., Sasselov D., 2011, ApJ, 736, L25
Kane S. R., Hinkel N. R., 2012, ApJ, 762, 7
Kasting J. F., Whitmire D. P., Reynolds R. T., 1993, Icarus, 101, 108
Kirkwood D., 1867, Meteoric Astronomy A Treatise On Shooting Stars, Fireballs and Aerolites. J.B. Lippincott & Co., Philadelphia
Kokubo E., Ida S., 1998, Icarus, 131, 171
Kokubo E., Ida S., 2000, Icarus, 143, 15

Kokubo E., Ida S., 2002, ApJ, 581, 666

Kopparapu R. K. et al., 2013a, ApJ, 765, 131

Kopparapu R. K. et al., 2013b, ApJ, 770, 82

Kostov V. B. et al., 2016, ApJ, 827, 86

Liberato L., Winter O. C., 2020, MNRAS, 496, 3700

Lissauer J. J., 1993, ARA&A, 31, 129

Lissauer J. J., Quintana E. V., Chambers J. E., Duncan M. J., Adams F. C., 2004, Rev. Mex. Astron. Astrofis., 22, 99

Liu H.-G., Zhang H., Zhou J.-L., 2013, ApJ, 767, L38

Mason P. A., Zuluaga J. I., Clark J. M., Cuartas-Restrepo P. A., 2013, ApJ, 774, L26

Mason P. A., Zuluaga J. I., Cuartas-Restrepo P. A., Clark J. M., 2015, Int. J. Astrobiol., 14, 391

Morishima R., Schmidt M. W., Stadel J., Moore B., 2008, ApJ, 685, 1247

Müller T. W., Haghighipour N., 2014, ApJ, 782, 26

Murray C. D., Dermott S. F., 1999, Solar System Dynamics. Cambridge Univ. Press, Cambridge

O'Brien D. P., Morbidelli A., Levison H. F., 2006, Icarus, 184, 39

Orosz J. A. et al., 2012a, Science, 337, 1511

Orosz J. A. et al., 2012b, ApJ, 758, 87

Orosz J. A. et al., 2019, AJ, 157, 174

Pichardo B., Sparke L. S., Aguilar L. A., 2005, MNRAS, 359, 521

Pichardo B., Sparke L. S., Aguilar L. A., 2008, MNRAS, 391, 815

Quarles B., Musielak Z. E., Cuntz M., 2012, ApJ, 750, 14

Quarles B., Satyal S., Kostov V., Kaib N., Haghighipour N., 2018, ApJ, 856, 150

Quintana E. V., Lissauer J. J., 2006, Icarus, 185, 1

Raymond S. N., Quinn T., Lunine J. I., 2005, ApJ, 632, 670

Safronov V. S., 1972, Evolution of the Protoplanetary Cloud and Formation of The Earth and Planets. Israel Program for Scientific Translations, Jerusalem

Schwarz R., Funk B., Zechner R., Bazsó Á., 2016, MNRAS, 460, 3598

Underwood D. R., Jones B. W., Sleep P. N., 2003, Int. J. Astrobiol., 2, 289

Welsh W. F. et al., 2012, Nature, 481, 475

Zuluaga J. I., Mason P. A., Cuartas-Restrepo P. A., 2016, ApJ, 818, 160

This paper has been typeset from a TEX/LATEX file prepared by the author.